Deacylation on the matrix side of the mitochondrial inner membrane regulates cardiolipin remodeling

Matthew G. Baile, Kevin Whited, and Steven M. Claypool
Department of Physiology, Johns Hopkins School of Medicine, Baltimore, MD 21205-2185

ABSTRACT **The mitochondrial-specific lipid cardiolipin (CL) is required for numerous processes therein. After its synthesis on the matrix-facing leaflet of the inner membrane (IM), CL undergoes acyl chain remodeling to achieve its final form. In yeast, this process is completed by the transacylase tafazzin, which associates with intermembrane space (IMS)-facing membrane leaflets. Mutations in *TAZ1* result in the X-linked cardiomyopathy Barth syndrome. Amazingly, despite this clear pathophysiological association, the physiological importance of CL remodeling is unresolved. In this paper, we show that the lipase initiating CL remodeling, Cld1p, is associated with the matrix-facing leaflet of the mitochondrial IM. Thus monolysocardiolipin generated by Cld1p must be transported to IMS-facing membrane leaflets to gain access to tafazzin, identifying a previously unknown step required for CL remodeling. Additionally, we show that Cld1p is the major site of regulation in CL remodeling; and that, like CL biosynthesis, CL remodeling is augmented in growth conditions requiring mitochondrially produced energy. However, unlike CL biosynthesis, dissipation of the mitochondrial membrane potential stimulates CL remodeling, identifying a novel feedback mechanism linking CL remodeling to oxidative phosphorylation capacity.**

Monitoring Editor
Benjamin S. Glick
University of Chicago

Received: Mar 6, 2013
Revised: Apr 17, 2013
Accepted: Apr 19, 2013

INTRODUCTION

Cardiolipin (CL) is a phospholipid unique to mitochondria that consists of two phosphatidyl head groups bridged by a glycerol, and four total fatty acyl chains (Schlame *et al.*, 2000). CL is important for numerous mitochondrial processes (Claypool and Koehler, 2012). It physically associates with, and enhances the function of, all major components of oxidative phosphorylation (OXPHOS; Fry and Green, 1980, 1981; Eble *et al.*, 1990; Gomez and Robinson, 1999; Sedlak and Robinson, 1999; Schwall *et al.*, 2012); promotes the stability of respiratory supercomplexes (Zhang *et al.*, 2002; Pfeiffer *et al.*, 2003; Brandner *et al.*, 2005; Zhang *et al.*, 2005; Claypool *et al.*, 2008b; Acehan *et al.*, 2011); is required for the optimal function of the mitochondrial fission and fusion machinery (DeVay *et al.*, 2009; Ban *et al.*, 2010; Montessuit *et al.*, 2010); is involved in protein import (Jiang *et al.*, 2000; van der Laan *et al.*, 2007; Gebert *et al.*, 2009; Marom *et al.*, 2009); and is implicated in apoptosis (Ostrander *et al.*, 2001; Gonzalvez *et al.*, 2008). While CL is required in mammals for life (Zhang *et al.*, 2011), it is nonessential in yeast (Jiang *et al.*, 1997; Tuller *et al.*, 1998). Nonetheless, yeast lacking CL display numerous defects, especially when grown in suboptimal conditions (Jiang *et al.*, 2000; Koshkin and Greenberg, 2000; Zhong *et al.*, 2004).

Eukaryotic CL biogenesis is evolutionarily conserved and only occurs within mitochondrial membranes (Schlame and Haldar, 1993). Despite the presence of CL on both leaflets of the inner membrane (IM) as well as on the outer membrane (OM; Petit *et al.*, 1994; Gebert *et al.*, 2009; Connerth *et al.*, 2013), newly synthesized CL is produced within the matrix-facing leaflet of the IM (Schlame and Haldar, 1993; Dzugasova *et al.*, 1998; Osman *et al.*, 2010). Thus the final distribution of CL within mitochondrial membranes must involve trafficking steps; however, the players and mechanisms responsible for these processes are presently unknown.

Furthermore, newly synthesized, immature CL, characterized by saturated acyl chains of variable length and asymmetry about the

This article was published online ahead of print in MBoC in Press (http://www.molbiolcell.org/cgi/doi/10.1091/mbc.E13-03-0121) on May 1, 2013.

Address correspondence to: Steven M. Claypool (sclaypo1@jhmi.edu).

Abbreviations used: CCCP, carbonyl cyanide *m*-chlorophenyl hydrazone; CL, cardiolipin; EV, empty vector; IM, inner membrane; IMS, intermembrane space; MLCL, monolysocardiolipin; OM, outer membrane; OXPHOS, oxidative phosphorylation; PK, proteinase K; ROS, reactive oxygen species.

central carbon of the bridging glycerol (Schlame *et al.*, 2005; Schlame and Ren, 2006), undergoes substantial acyl chain remodeling. CL remodeling is initiated by a phospholipase that removes an acyl chain forming monolysocardiolipin (MLCL); MLCL is then reacylated by an acyltransferase or a transacylase to form mature CL, characterized by unsaturated acyl chains and a high degree of molecular symmetry (Schlame *et al.*, 2005; Claypool and Koehler, 2012).

At least three distinct CL remodeling pathways may exist in mammals. Interestingly, all three implicated CL remodeling enzymes are located in separate compartments. MLCL acyltransferase 1 resides on the inner leaflet of the IM (Taylor and Hatch, 2009), and acyl-CoA:lysocardiolipin acyltransferase 1 is located in the mitochondria-associated membrane compartment of the endoplasmic reticulum (ER; Li *et al.*, 2010). Tafazzin (Taz1p in yeast), the only CL remodeling enzyme identified in yeast (Claypool and Koehler, 2012), is an MLCL transacylase that removes an acyl chain from another phospholipid (preferentially phosphatidylcholine or phosphatidylethanolamine) and adds it to MLCL, thus regenerating CL (Xu *et al.*, 2003, 2006). It is an interfacial membrane protein that resides in the intermembrane space (IMS)-facing leaflet of both the IM and OM (Claypool *et al.*, 2006). Therefore CL remodeling must involve not only the transbilayer movement of CL and/or its derivatives but, additionally, trafficking between the IM and OM and the mitochondrion and the ER. Nothing is currently known about any of these processes.

Mutations in *TAZ1* cause the X-linked disease, Barth syndrome, which is clinically characterized by cardiomyopathy, skeletal myopathy, growth retardation, and cyclical neutropenia (Barth *et al.*, 1983; Bione *et al.*, 1996; Schlame and Ren, 2006). Mitochondria from Barth syndrome patients exhibit abnormal ultrastructure accompanied by variable respiratory chain defects (Barth *et al.*, 1983; Acehan *et al.*, 2007, 2009). In Barth syndrome, CL levels are decreased with a concurrent increase in MLCL, and the acyl chain composition of CL is abnormal (Schlame *et al.*, 2003; Valianpour *et al.*, 2005). Combined, these observations suggest that CL remodeling is required for optimal mitochondrial function (Schlame *et al.*, 2005; Cheng *et al.*, 2008; Claypool and Koehler, 2012).

One approach toward delineating the trafficking steps required for the biosynthesis of phospholipids is to define the subcellular localization and membrane topology of every participating enzyme. As one example, the localization of Cho1p/Pss1p to the ER and the mitochondrial Psd1p to the mitochondrial IM demonstrated that phosphatidylserine produced in the ER must traffic from the ER to the OM and finally to the IM to be decarboxylated to phosphatidylethanolamine (Kuge and Nishijima, 2003; Voelker, 2005; Horvath *et al.*, 2012; Tamura *et al.*, 2012). Thus basic cell biological information outlined the steps required for the mitochondrial production of phosphatidylethanolamine. Importantly, such information also provided insight into the regulation of mitochondrial phosphatidylethanolamine production (Kuge and Nishijima, 2003).

The pathophysiological importance of the tafazzin-mediated CL remodeling pathway is firmly established (Bione *et al.*, 1996; Schlame and Ren, 2006). In contrast, the contribution of CL remodeling to physiology is perhaps surprisingly unresolved. In large part, this reflects the absence of any information concerning whether and how the tafazzin-mediated CL remodeling pathway is regulated. A major obstacle preventing a detailed investigation into the regulation of the tafazzin-mediated CL remodeling pathway is the absence of any basic cell biological information about the lipase that functions upstream of tafazzin and initiates the CL remodeling process. As such, we sought here to characterize CL-specific deacylase 1 (Cld1p), the phospholipase that initiates CL remodeling in yeast (Beranek *et al.*, 2009), in an effort to define the trafficking steps required for tafazzin-mediated CL remodeling and gain insight into the regulation of this process. We show that endogenous Cld1p is embedded in the matrix-facing leaflet of the IM, the opposite side of the IM as Taz1p. The nonintegral nature of Cld1p's membrane association indicates that Cld1p-mediated deacylation of CL to MLCL is not directly coupled to the flipping of MLCL to the IMS-facing leaflet of the IM. This in turn suggests the existence of an as yet unidentified protein(s) capable of redistributing MLCL, and possibly CL, between leaflets of the IM. Finally, we investigated the regulation of CL remodeling and demonstrate that Cld1p is the key step that controls the tafazzin-mediated CL remodeling pathway. Interestingly, disruption of the electrochemical gradient across the IM increases Cld1p function suggesting a novel mechanism by which mitochondria are able to respond to insufficient energy production by generating a form of CL that promotes and/or preserves OXPHOS capacity.

RESULTS

Cld1p resides in the mitochondrial IM

Analysis of mitochondrial phospholipids indicates that Cld1p functions upstream of Taz1p in CL remodeling; however, the growth phenotypes of Δ*taz1*, Δ*cld1*, and Δ*taz1*Δ*cld1* on respiratory media suggest that Cld1p may also participate in a separate pathway (Beranek *et al.*, 2009). Thus the subcellular localization of endogenous Cld1p was analyzed. Consistent with the localization of Cld1p–green fluorescent protein (Beranek *et al.*, 2009), endogenous Cld1p cofractionated entirely with the mitochondrial marker, Qcr6p (Figure 1A) and is therefore exclusively localized to mitochondria.

Because CL remodeling is topologically complex (Claypool and Koehler, 2012), the submitochondrial localization of Cld1p was examined. First, we took advantage of the fact that varying concentrations of digitonin are able to selectively solubilize different mitochondrial compartments (Glick *et al.*, 1992; Tamura *et al.*, 2012). At very low concentrations of digitonin, the OM is permeabilized, releasing soluble IMS proteins (Figure 1, B and C). As the digitonin concentration increases, the IM becomes permeabilized, releasing soluble matrix proteins; this is followed by the solubilization and release of membrane-associated OM proteins and, finally, IM proteins. The fractionation profile of Cld1p is similar to that of the IM marker proteins, indicating that Cld1p localizes to the IM.

To determine the side of the IM on which Cld1p is located, we examined the protease accessibility of Cld1p in intact mitochondria, mitoplasts generated by osmotically rupturing the OM, and deoxycholate-solubilized mitochondrial extracts. Cld1p was protected from the protease, unless the IM was solubilized, similar to the matrix protein Kgd1p, and unlike Tom70p, which faces the cytosol, or Taz1p and Dld1p, which face the IMS (Figure 1D). This supports the IM localization of Cld1p and additionally indicates that it either faces the matrix or, if it is a membrane-spanning protein, contains an IMS-facing, protease-resistant domain.

Cld1p is associated with the matrix-facing leaflet of the IM

Protein topology prediction programs vary in their assessment of Cld1p, predicting no, one, or two transmembrane domains (Supplemental Table S1). Therefore the submitochondrial localization of each terminus of Cld1p was assessed by protease protection. Cld1p with a 10xHis + protein C epitope tags (CNAP tag; Claypool *et al.*, 2008b) on either the predicted mature N-terminus (after aa 41) or the C-terminus were transformed into Δ*cld1*Δ*taz1* yeast to test their physiological relevance. In Δ*taz1* yeast, MLCL accumulates at the expense of CL, whereas in Δ*cld1* and Δ*cld1*Δ*taz1* yeast, CL levels are

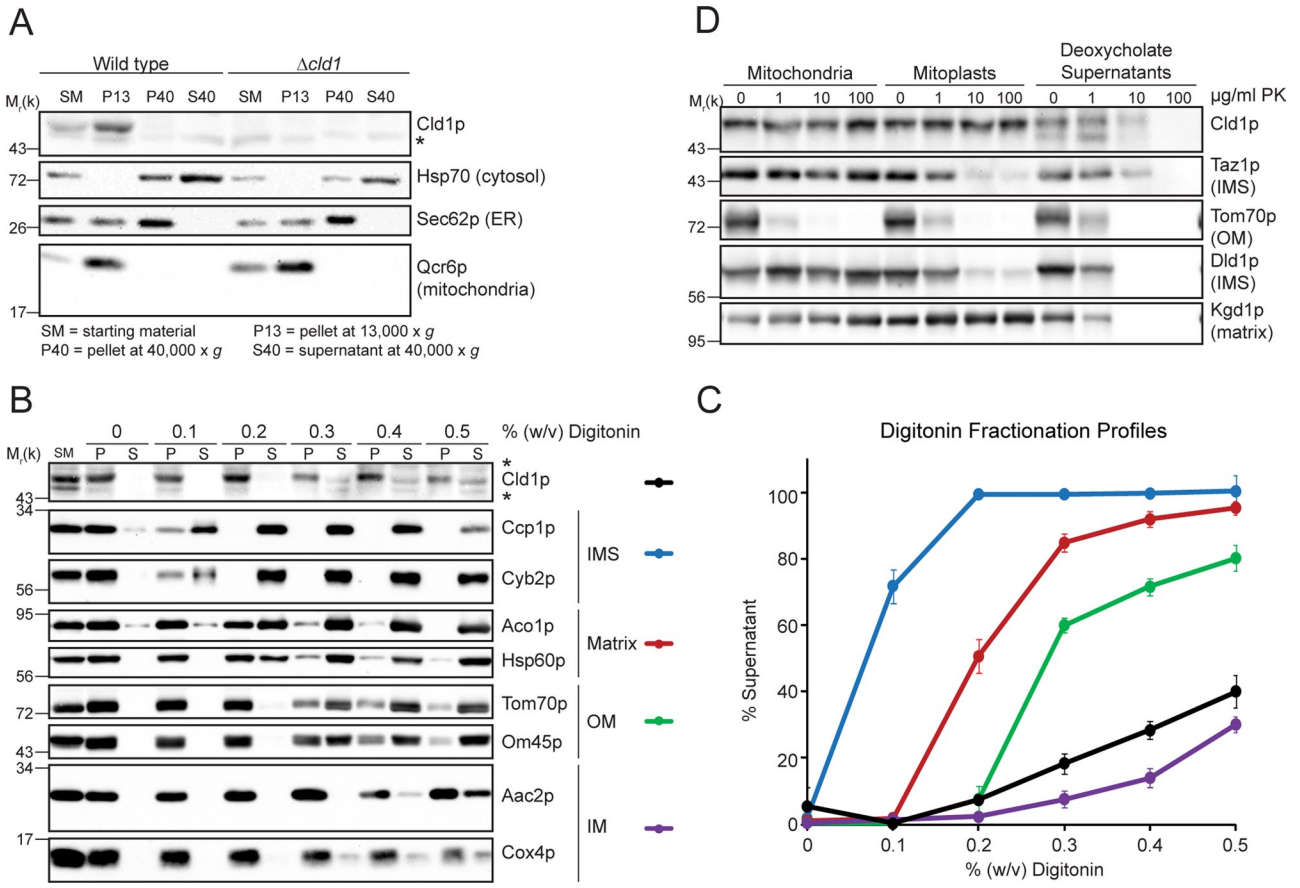

FIGURE 1: Cld1p resides in the mitochondrial IM. (A) Yeast subcellular fractions were prepared by differential centrifugation. Fifty micrograms (for Cld1p) or 25 µg (for all other proteins) of each fraction was separated by SDS–PAGE and immunoblotted as indicated. (B and C) Mitochondria isolated from wild-type yeast were solubilized with the indicated concentration of digitonin. (B) Equal volumes of extracted (S) and nonextracted (P) protein for each digitonin concentration were separated by SDS–PAGE and immunoblotted. (C) The band intensities for two markers per compartment were combined and plotted as the percent of signal in the supernatant (mean ± SEM; $n = 3$). (D) Intact mitochondria, mitoplasts, or deoxycholate-solubilized mitochondria from wild-type yeast were incubated with the indicated concentrations of proteinase k (PK), and 50 µg of each sample was separated by SDS–PAGE and immunoblotted as indicated. *, nonspecific cross-reaction of the Cld1p antiserum.

normal (Beranek *et al.*, 2009). Thus, if Δ*cld1*Δ*taz1* yeast are rescued with a functional Cld1p, MLCL will accumulate. Both tagged forms of Cld1p were expressed (Figure 2A) and resulted in the accumulation of MLCL (Figure 2B), indicating that the addition of the CNAP tag to either terminus did not preclude function.

The CNAP tag was only degraded by the protease after the addition of detergent, regardless of its location on the mature N- or C-terminus (Figure 2, C and D). Thus both termini face the matrix, consistent with Cld1p containing no or an even number of transmembrane domains.

To experimentally determine whether Cld1p is a peripheral or integral membrane protein, mitochondria were incubated in 0.1 M carbonate at increasing pH. After ultracentrifugation, the integral membrane protein Pic1p remained associated with the membrane pellet, while the peripheral membrane protein Cyc1p was released into the supernatant at every tested pH (Figure 3, A and B). Cld1p was partially released from the membrane at pH 10.5, and was further extracted as the pH increased. This extraction profile, intermediate to either integral membrane proteins or peripheral proteins, suggests that Cld1p is an interfacial membrane protein, containing segments that extend into, but not completely through, the membrane.

The membrane association of Cld1p was further analyzed by sonication (Figure 3C). Mitoplasts were incubated with various concentrations of KCl. After removal of the IMS proteins, mitoplasts were resuspended in buffer containing the same concentrations of KCl and subjected to sonication. Membrane-bound proteins were then separated from released proteins by ultracentrifugation. As expected, the soluble IMS protein Cyb2p was released from mitoplasts, regardless of the KCl concentration (Figure 3D). Cyc1p on the other hand, which is peripherally attached to the IMS-facing leaflet of the IM, remained bound to mitoplasts when no KCl was added but was released as the KCl concentration increased. The integral membrane proteins Rip1p and Aac2p remained associated with the membrane pellet after sonication, whereas the soluble matrix protein Aco1p was released after sonication. Upon sonication, in the absence of KCl, Cld1p remained completely membrane bound but was released in a salt-titratable manner. Therefore electrostatic interactions at least partially define Cld1p membrane association. However, that a small amount of Cld1p remained membrane bound even at very high salt concentrations indicates that electrostatic interactions are not the only determinant of its membrane association. Importantly, Cld1p was never detected in the IMS fractions,

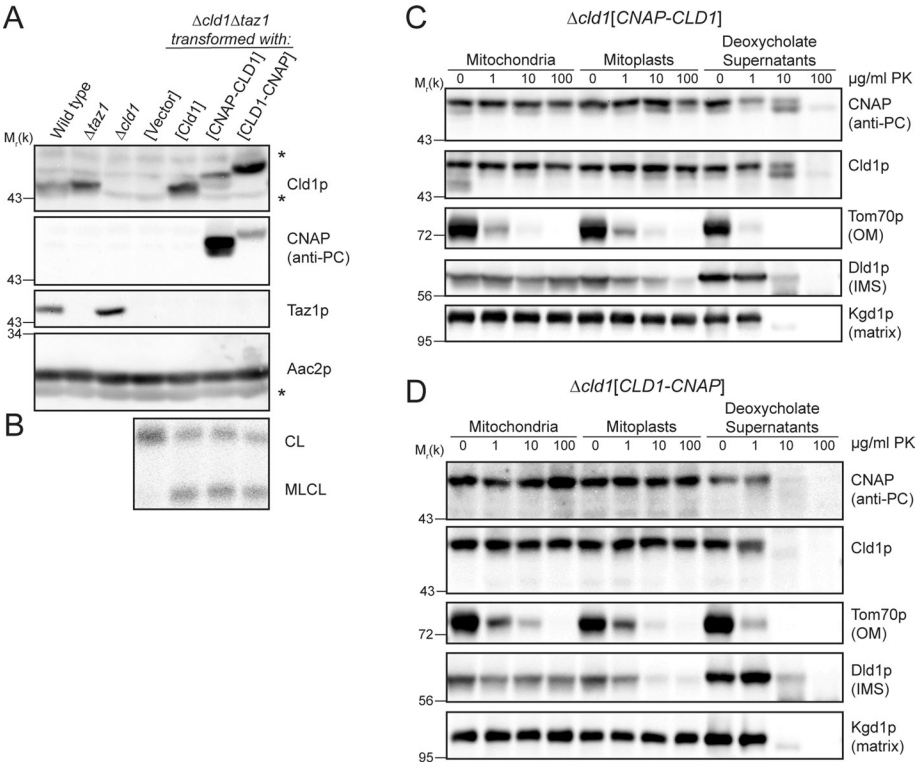

FIGURE 2: Both termini of Cld1p face the matrix. (A) Whole-cell extracts were separated by SDS–PAGE and immunoblotted as indicated. *, a nonspecific cross-reaction of the Cld1p antiserum. (B) Mitochondrial phospholipids from the indicated strains were labeled with $^{32}P_i$ and separated by thin-layer chromatography (TLC). (C and D) Intact mitochondria, mitoplasts, or deoxycholate-solubilized mitochondria from Δ*cld1* yeast transformed with (C) *CNAP-CLD1* or (D) *CLD1-CNAP* were incubated with the indicated concentrations of PK, and 50 μg of each sample were separated by SDS–PAGE and immunoblotted as indicated.

regardless of the inclusion of KCl. Thus the ability of salt to release Cld1p from the IM only after sonication confirms that Cld1p associates with the matrix-facing leaflet of the IM. Together with the localization of the N- and C-termini of Cld1p, these results indicate that Cld1p associates with membranes but lacks canonical membrane-spanning segments.

The membrane association of Cld1p is enhanced by its substrate

The role of CL in the membrane association of Cld1p was next tested in mitochondria lacking CL synthase (Δ*crd1*), and thus CL. After sonication, Cld1p remained mostly membrane bound in the absence of KCl, even in Δ*crd1* mitochondria (Figure 3, E and F). However, at both 100 and 250 mM KCl, Cld1p was extracted more readily from mitochondria lacking CL, suggesting that CL facilitates Cld1p's membrane association. However, when analyzed by carbonate extraction, the extraction profile of Cld1p was similar in both wild-type and Δ*crd1* mitochondria, except at pH 10.5, at which Cld1p was slightly more extractable in the absence of CL (Figure 3, A and B). Thus Cld1p still acts as an interfacial membrane protein, even in the absence of CL. Taken together, these data indicate that Cld1p bound to the IM via residues that extend into, but not through, the membrane independent of CL, but that CL contributes to the electrostatic interaction of Cld1p with the IM (Figure 3G).

The catalytic triad of Cld1p

Two motifs were predicted to be involved in Cld1p function (Beranek *et al.*, 2009): the AXSXG motif, of which the serine residue is expected to be critical for lipase or acyltransferase activity, and the HX_4D motif, a conserved structural motif in acyltransferases (Figure 4A). However, the requirement for either of these motifs has not been formally tested. Sequence analysis of Cld1p predicts that the C-terminus contains an α/β-hydrolase fold (Beranek *et al.*, 2009), a family of enzymes with diverse substrate specificity but that invariably contain a catalytic triad consisting of a nucleophile, an acidic residue, and a histidine (Holmquist, 2000).

For identification of the catalytic residues, a homology model of the α/β-hydrolase domain was generated (Figure 4B) using the α/β-hydrolase domain–containing CumD as a template (Fushinobu *et al.*, 2002). The predicted nucleophile, Ser-230, of the AXSXG motif and residues within the HX_4D motif were individually mutated, as well as additional potential catalytic residues identified by their location within the homology model (Figure 4, A and B). Each Cld1p mutant was expressed after being transformed into Δ*cld1*Δ*taz1* yeast, and its function was analyzed by measuring the accumulation of MLCL (Figure 4, C and D). Mutating Ser-230 or His-424 to alanine inactivated Cld1p. His-424 is predicted to be adjacent to the catalytic serine residue, consistent with its participation in catalysis. In contrast, mutating Asp-429 within the HX_4D motif did not ablate Cld1p function, indicating this motif may not be a bona fide transacylase motif. Instead, mutating Asp-392, one of four additional aspartic acid residues adjacent to the catalytic pocket identified in the homology model, to asparagine abolished Cld1p activity. Importantly, mutating Ser-230, His-424, or Asp-429 did not affect Cld1p assembly (Figure 5A), suggesting that the lack of Cld1p activity is not due to overall protein misfolding. Thus Ser-230, His-424, and Asp-392 compose the catalytic triad of Cld1p.

Cld1p functions as a monomer

The α/β-hydrolase fold family of proteins contains enzymes that exist as monomers or higher oligomers (Kim *et al.*, 1997; Carr and Ollis, 2009; Thoms *et al.*, 2011). Analysis by two-dimensional blue native/SDS–PAGE reveals that the majority of Cld1p migrates between 80 and 120 kDa, but higher-molecular-weight complexes are also present (Figure 5A), suggesting dimerization or higher oligomerization. We sought to determine whether this potential oligomerization is required for Cld1p activity by testing whether a Cld1p catalytic mutant functions as a dominant negative. When expressed in a Δ*taz1* strain (which contains endogenous Cld1p), a dominant negative allele should inhibit the function of endogenous Cld1p, resulting in decreased MLCL and increased CL compared with Δ*taz1*. Wild-type or the H424A Cld1p mutant were expressed from low- (centromeric, ↑) or high- (2 μm, ↑↑) copy plasmids in a Δ*taz1* strain (Figure 5B). However, phospholipid analysis showed no difference in the levels of CL and MLCL compared with Δ*taz1* rescued with empty vector (EV; Figure 5C). Therefore, despite Cld1p's participation in higher-order assemblies (either

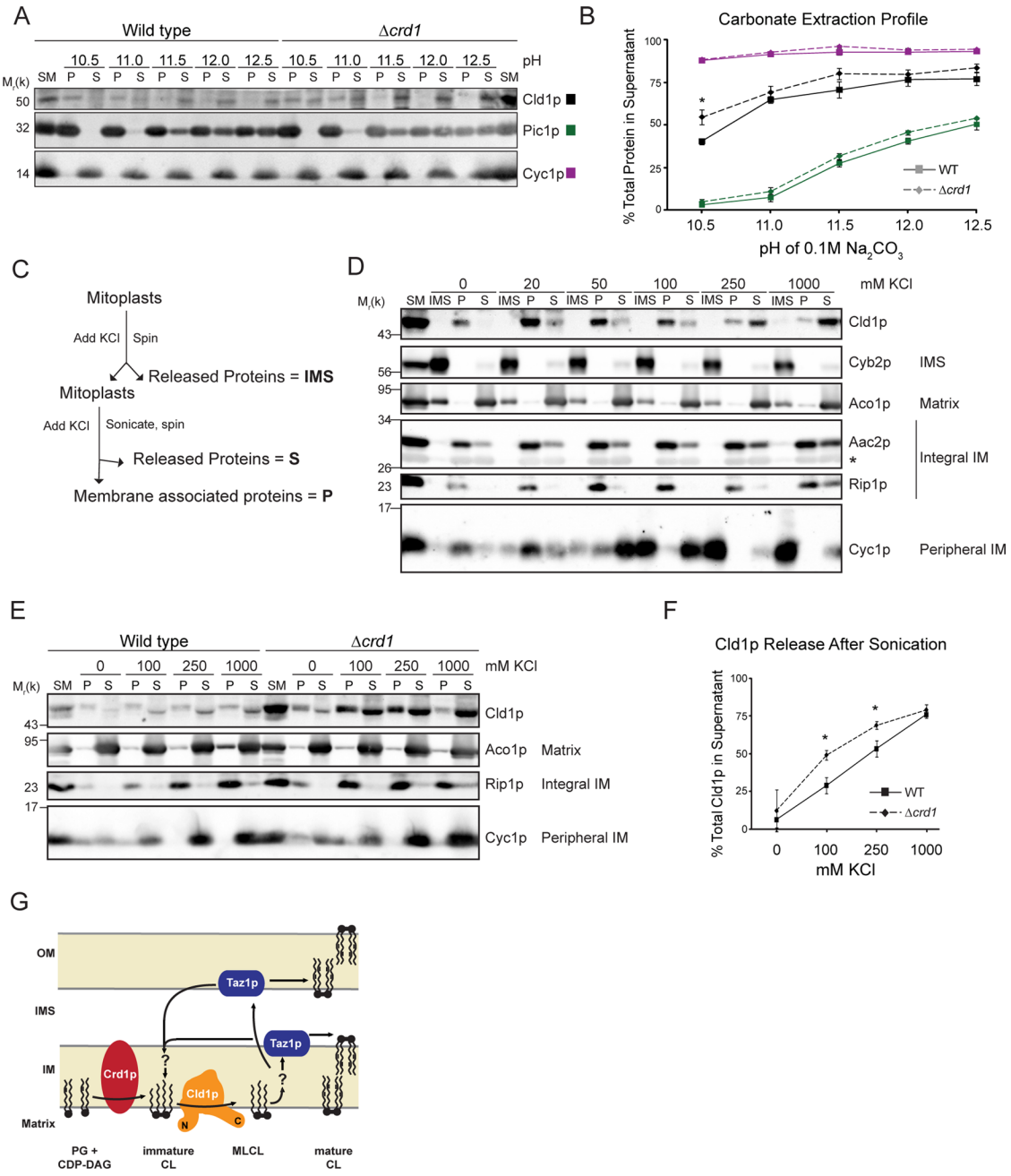

FIGURE 3: Cld1p is associated with the matrix-facing leaflet of the IM. (A) Wild-type or Δ*crd1* mitochondria were incubated in 0.1 M carbonate of the indicated pH. Membrane-bound proteins (P) were separated from released proteins (S) by ultracentrifugation, and equal volumes of each fraction were resolved by SDS–PAGE and immunoblotted as indicated. (B) Band intensities of the P and S fractions were quantified and plotted as the percentage of total protein released into the supernatant for each pH (mean ± SEM; $n = 4$). Solid and dashed lines indicate wild-type and Δ*crd1* mitochondria, respectively. (C) Outline of the sonication experiment in (D). (D) Wild-type mitoplasts were incubated with the indicated concentration of KCl, and pelleted by centrifugation. Released proteins (IMS) in the supernatant were removed and TCA-precipitated. Mitoplasts were resuspended in buffer maintaining the indicated KCl concentration and sonicated. Membranes (P) were separated from released proteins (S) by ultracentrifugation. Equal amounts of each sample were resolved by SDS–PAGE and immunoblotted as indicated. (E) Intact wild-type or Δ*crd1* mitochondria were sonicated in the presence of the indicated KCl concentrations as in (D). (F) Band intensities of the P and S fractions were quantified and plotted as the percentage of total protein released into the supernatant for each KCl concentration (mean ± SEM; $n = 4$). (G) Cld1p is embedded in the IM facing the mitochondrial matrix. (B and F) *, a statistically significant difference ($p < 0.05$) as determined by *t* test.

with itself, other proteins, or phospholipids), oligomerization is not required for Cld1p function, indicating that the functional unit is likely a monomer.

Cld1p is up-regulated during respiratory conditions

The regulation of CL remodeling has not been documented. To this end, the steady-state expression of Cld1p and Taz1p, and CL and

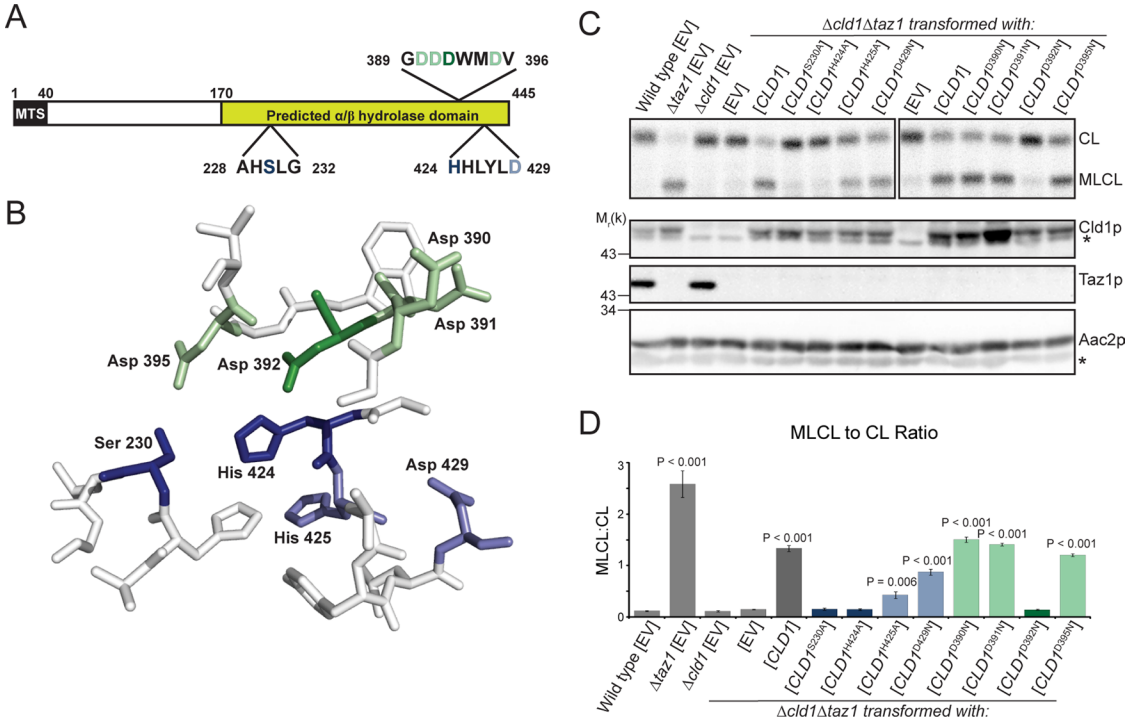

FIGURE 4: The catalytic triad of Cld1p. (A) Schematic of Cld1p, containing a predicted mitochondrial targeting sequence (MTS) and α/β-hydrolase domain. Amino acid residues mutated in the predicted lipase motif (residues 228–232) and acyltransferase structural motif (residues 424–429) are shown in blue with additional mutated residues in green. (B) The α/β-hydrolase domain of Cld1p was modeled with SWISS-MODEL. Residues constituting the predicted catalytic pocket of Cld1p are shown and colored as in (A). (C) Mitochondrial phospholipids from the indicated strains were labeled with $^{32}P_i$ and separated by TLC (top panel). Whole-cell extracts were immunoblotted as indicated (bottom panels). (D) Quantification of the MLCL:CL ratio (mean ± SEM; $n = 6$). Significant differences compared with Δ*cld1*Δ*taz1*[EV] were determined by one-way ANOVA. *, nonspecific bands.

MLCL levels, in yeast grown in various carbon sources were examined. In dextrose, which represses proteins involved in mitochondrial-mediated metabolism (Ohlmeier *et al.*, 2004), Cld1p was barely detectable, whereas in raffinose, a fermentable carbon source that does not result in glucose repression, Cld1p was expressed at higher levels. Cld1p and Taz1p expression was highest when yeast were grown in the nonfermentable carbon source, lactate (Figure 6, A and B). Importantly, no differences in expression were observed between wild-type, Δ*cld1*, and Δ*taz1* yeast grown in the same media (Supplemental Figure S1), indicating that the presence of a functional remodeling pathway does not regulate the expression of Cld1p or Taz1p.

Analysis of mitochondrial phospholipids revealed that the sum of CL + MLCL, a gauge of CL biosynthesis that is equivalent for wild-type, Δ*cld1*, and Δ*taz1* mutants, is reduced in yeast grown in dextrose compared with raffinose or rich lactate (Figures 6, C and D, and S2), consistent with previous studies of CL biosynthesis (Shen and Dowhan, 1998; Gu *et al.*, 2004; Su and Dowhan, 2006; Chen *et al.*, 2008; Claypool *et al.*, 2008a). Similar to the steady-state expression, no differences are observed in CL + MLCL levels between wild-type, Δ*cld1*, or Δ*taz1* yeast grown in the same media (Figure 6D), demonstrating that CL biosynthesis is not affected by defects in the CL remodeling pathway.

In Δ*taz1* yeast, the ratio of the accumulated MLCL to CL provides a means to determine the function of Cld1p. In the absence of Taz1p, MLCL generated by Cld1p cannot be reacylated and thus accumulates. The MLCL:CL ratio in Δ*taz1* yeast, and therefore the function of Cld1p, is lowest in the presence of dextrose and highest in the presence of lactate (Figure 6E), correlating with the steady-state expression levels of Cld1p (Figure 6B).

For further examination of how Cld1p expression levels affect its function, Cld1p was overexpressed in Δ*taz1* yeast. Expression of *CLD1* from a centromeric plasmid resulted in similar increases in Cld1p steady-state expression compared with endogenous Cld1p in each media type (2.6-fold higher in both dextrose and raffinose; 2.9-fold higher in lactate; Figure 7, A and B). Overexpression of Cld1p did not alter the total amount of CL + MLCL (Figure 7, C and D), although CL was significantly decreased in lactate-containing media (Figure S3A), and MLCL was significantly increased in raffinose-containing media (Figure S3B). In all media types, the MLCL:CL ratio was slightly but significantly increased when Cld1p was overexpressed (Figure 7E), although to a lesser extent than expected based on the degree of overexpression (compare Δ*taz1* [EV] in rich lactate and Δ*taz1* [*CLD1*] in raffinose), which suggests that factors other than simply steady-state abundance regulate Cld1p function.

Cld1p function is enhanced after dissipation of the mitochondrial membrane potential

To gain further insight into the regulation of CL remodeling, we examined the CL and MLCL levels in yeast treated with mitochondrial ionophores. CL biosynthesis has been shown to decrease when the mitochondrial pH gradient is dissipated with carbonyl cyanide *m*-chlorophenyl hydrazone (CCCP), but not when the membrane potential is ablated with valinomycin (Gohil *et al.*, 2004); however, the role of the electrochemical gradient in regulating CL remodeling has never been tested. CCCP (20 μM) and valinomycin (1 μM) inhibited growth in lactate-containing media, but had no effect on cell growth in media containing raffinose as the carbon source (Figure S4, A and B). Steady-state levels of mitochondrial phospholipids were

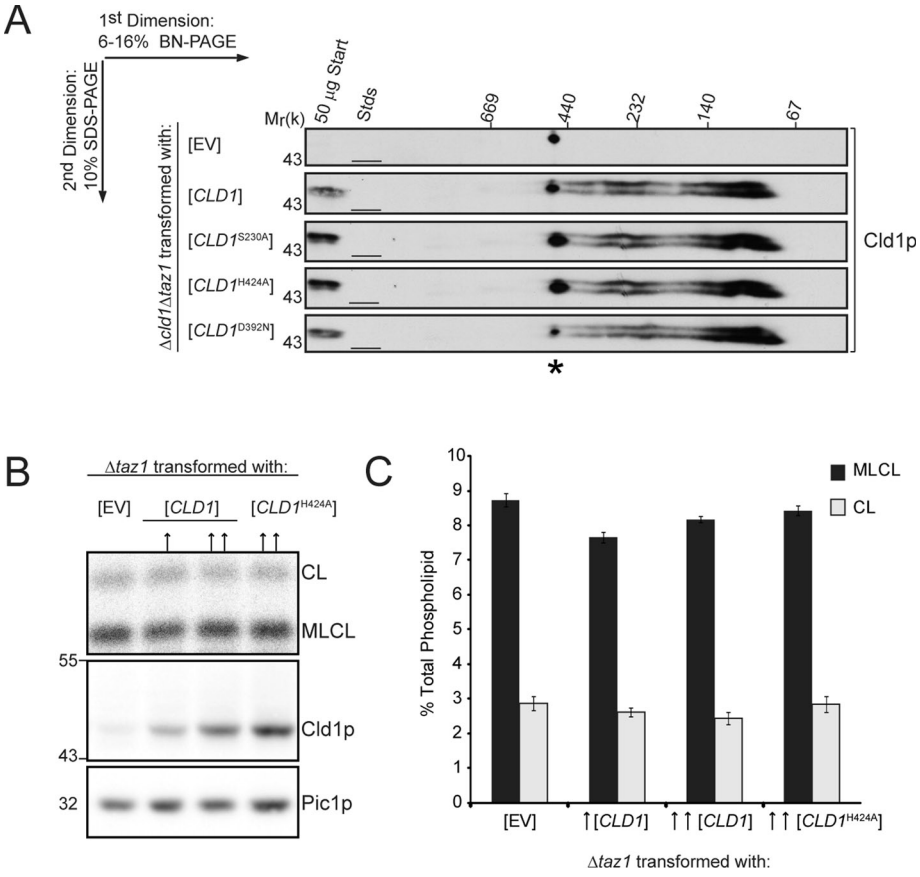

FIGURE 5: Cld1p functions as a monomer. (A) Mitochondria (150 μg) isolated from the indicated strains were solubilized with 1.5% (wt/vol) digitonin, separated by two-dimensional blue native/SDS–PAGE, and immunoblotted for Cld1p. *, a nonspecific cross-reaction of the Cld1p antiserum. (B) Mitochondrial phospholipids from the indicated strains were labeled with $^{32}P_i$ and separated by TLC (top panel). Whole-cell extracts from the indicated strains were resolved by SDS–PAGE and immunoblotted for Cld1p and the loading control Pic1p (bottom panels). ↑, a low copy (centromeric) plasmid; ↑↑, a high copy (2 μm) plasmid. (C) Quantification of CL and MLCL (mean ± SEM; $n = 6$).

analyzed after treatment for 24 h in raffinose-containing media (Figure 8, A and B). The levels of CL + MLCL in wild-type yeast were not significantly affected by treatment with either CCCP or valinomycin, demonstrating that CL biosynthesis is not affected by chronic disruption of the mitochondrial membrane potential or pH gradient. Treatment with CCCP or valinomycin did not affect the total levels of CL + MLCL in either mutant, indicating that defects in the remodeling pathway compounded with sustained dissipation of the electrochemical gradient do not affect CL biosynthesis. The MLCL:CL ratio in Δ*taz1* yeast increased after treatment with either CCCP or valinomycin (Figure 8C), signifying that Cld1p function is enhanced in the absence of a membrane potential. This increase in function is not due to an increase in Cld1p expression (Figure 8, D and E), suggesting that the increased MLCL:CL ratio is due to increased Cld1p activity. Of note, Taz1p expression did increase after treatment with the ionophores (Figure S4C), indicating that regulation of its expression is independent of Cld1p expression.

DISCUSSION

A new step required for CL remodeling

While much is known about the enzymatic reactions involved in the biosynthesis and remodeling of CL, relatively little is known about CL trafficking. Namely, how does immature CL synthesized on the matrix-facing leaflet of the IM gain access to tafazzin on the IMS-facing leaflets of the inner and outer membranes to complete CL remodeling? To begin to answer this question, we determined the submitochondrial localization and membrane association of Cld1p, the lipase that initiates CL remodeling. In this study, we have shown that Cld1p is embedded in the IM but does not span through it to the IMS. Because Cld1p in Δ*crd1* mitochondria remained membrane bound in the absence of added salt after sonication, and its carbonate extraction profile did not change at a higher pH compared with wild-type, it is unlikely that Cld1p is simply tethered to the membrane by CL. Rather, that Cld1p is more readily extracted by salt in the absence of CL suggests that its electrostatic interaction with the membrane is, at least partially, via the negatively charged head group of its substrate, CL.

The nature of Cld1p's membrane association is consistent with its function as a CL deacylase. Similar to the interfacial membrane protein Taz1p (Claypool *et al.*, 2006), Cld1p must catalyze a reaction within the membrane bilayer, at the interface between the hydrophilic head groups and hydrophobic fatty-acyl chains. This is in contrast to an enzyme that catalyzes a reaction on the head group of a phospholipid, such as Gep4p, which dephosphorylates phosphatidylglycerolphosphate to phosphatidylglycerol and is only peripherally attached to the IM (Osman *et al.*, 2010).

The enzymatic activity of Crd1p (Schlame and Haldar, 1993) also occurs on the matrix-facing leaflet of the IM, suggesting that, after synthesis, CL is deacylated by Cld1p forming MLCL, and that MLCL is the phospholipid that must be transported across the IM to Taz1p-containing membranes to complete CL remodeling (Figure 3G). Because Cld1p does not span the IM, its enzymatic activity is not coupled to the flipping of MLCL to the IMS-facing leaflet of the IM. The generation of mature CL requires multiple rounds of deacylation and reacylation. Consequently, after MLCL is translocated to Taz1p-containing leaflets for reacylation, newly reacylated CL may need to traffic back to the matrix-facing leaflet of the IM to become available for Cld1p to remove another acyl chain—a cycle that would repeat until mature CL is generated. However, Taz1p-mediated transacylation requires only a phospholipid and a lysophospholipid (Malhotra *et al.*, 2009) in the context of a curved membrane (Schlame *et al.*, 2012). It is therefore possible that the lysophospholipid generated after the first reacylation of CL is used as an acyl chain acceptor for Taz1p to subsequently rederive MLCL from CL. Thus, after Cld1p initiates CL remodeling by generating MLCL on the matrix-facing leaflet of the IM, the subsequent acylation/deacylation reactions would be mediated solely by Taz1p via transacylation and occur within the same leaflet. In either scenario, after Cld1p initiates CL remodeling by generating MLCL, an as yet unidentified protein(s) must mediate the redistribution of MLCL to the IMS-facing leaflets of the inner and outer membranes.

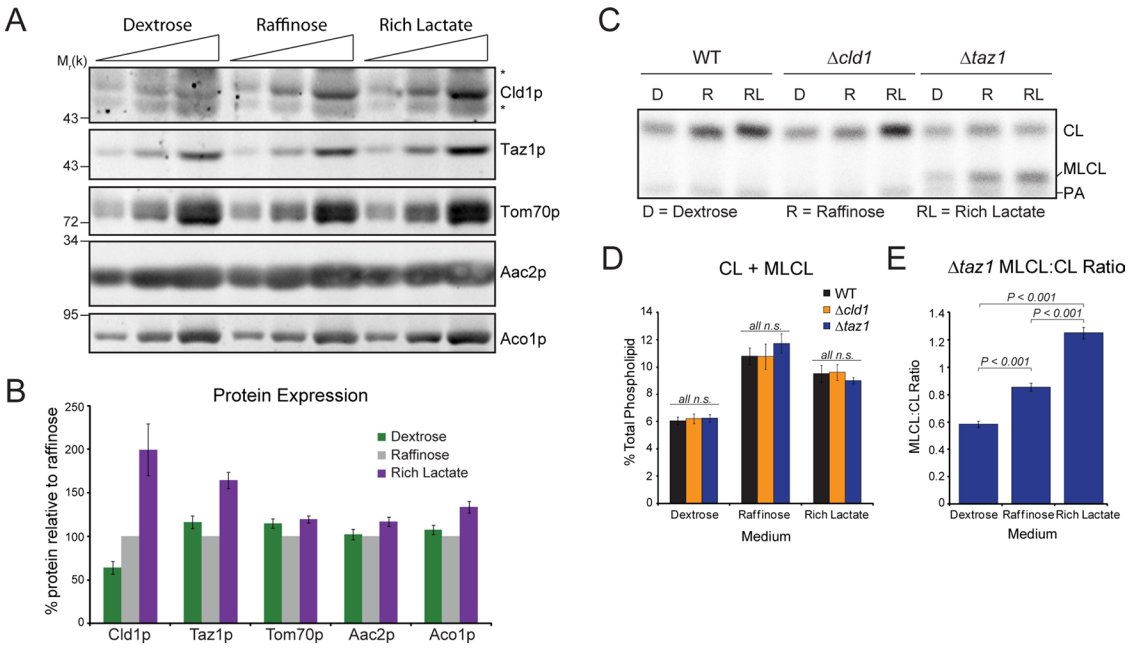

FIGURE 6: Cld1p expression and function is modulated by the available carbon source. (A) Whole-cell extracts from wild-type yeast grown in YP-dextrose (Dextrose), YP-raffinose (Raffinose), or rich lactate were resolved by SDS–PAGE and immunoblotted as indicated. *, nonspecific cross-reactions of the Cld1p antiserum. (B) Band intensities from wild-type yeast were quantified and expressed as the % protein relative to raffinose (mean ± SEM; $n = 17$). (C) Mitochondrial phospholipids from yeast grown in the indicated media were labeled with $^{32}P_i$ and separated by TLC. (D) The sum of CL + MLCL from the indicated strains (mean ± SEM; $n = 6$). n.s., differences not significant. (E) The ratio of MLCL:CL from Δ*taz1* (mean ± SEM; $n = 6$). Significant differences determined by one-way ANOVA.

Is there any attractive candidate(s) for this novel activity? The simple answer is no. While proteins mediating phospholipid redistribution between membrane leaflets have been identified for the plasma membrane, ER, Golgi, and endosomes (van Meer *et al.*, 2008), little is known about phospholipid trafficking in the mitochondrion. CL redistribution between IM leaflets has been demonstrated

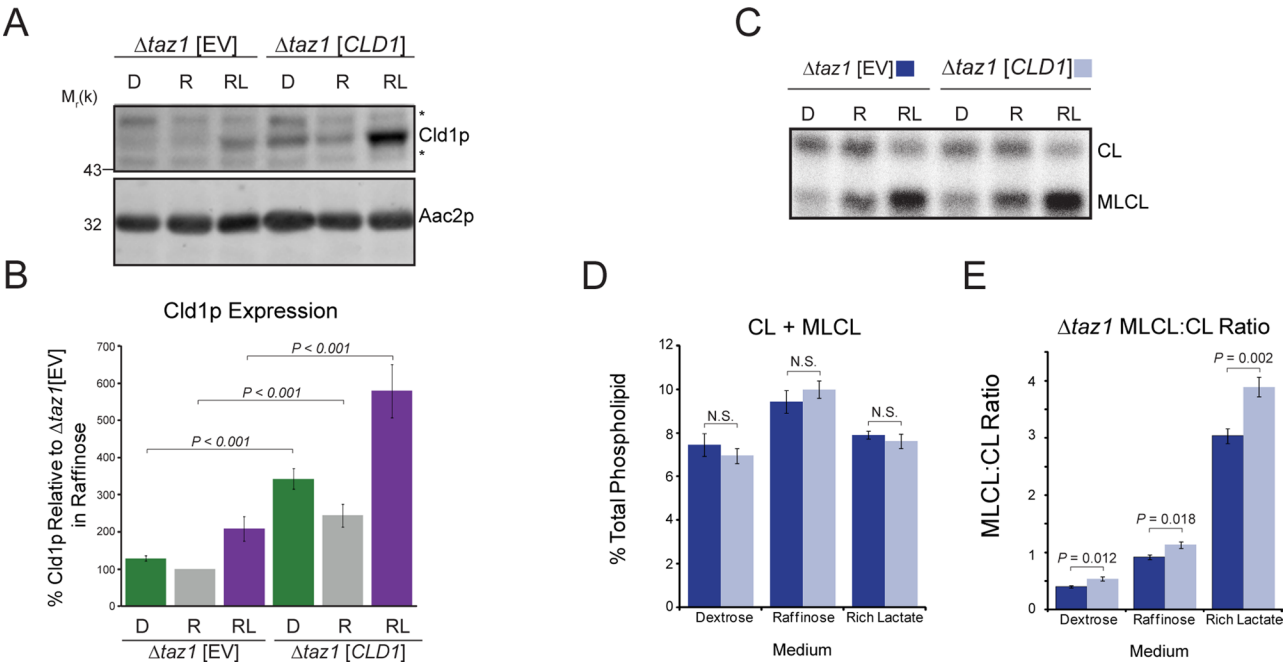

FIGURE 7: Cld1p overexpression does not cause a proportional increase in function. (A) Whole-cell extracts from Δ*taz1* yeast transformed with an EV or *CLD1* grown in YP-dextrose (D), YP-raffinose (R), or rich lactate (RL) were separated by SDS–PAGE and immunoblotted as indicated. *, nonspecific cross-reactions of the Cld1p antiserum. (B) Cld1p band intensities were quantified and plotted as the % protein relative to Δ*taz1*[EV] grown in raffinose (mean ± SEM; $n = 8$). (C) Mitochondrial phospholipids from yeast grown in the indicated media were labeled with $^{32}P_i$ and separated by TLC. (D) The sum of CL + MLCL from the indicated strains (mean ± SEM; $n = 6$). n.s., differences not significant. (E) The ratio of MLCL:CL from Δ*taz1* (mean ± SEM; $n = 6$). Significant differences determined by *t* test.

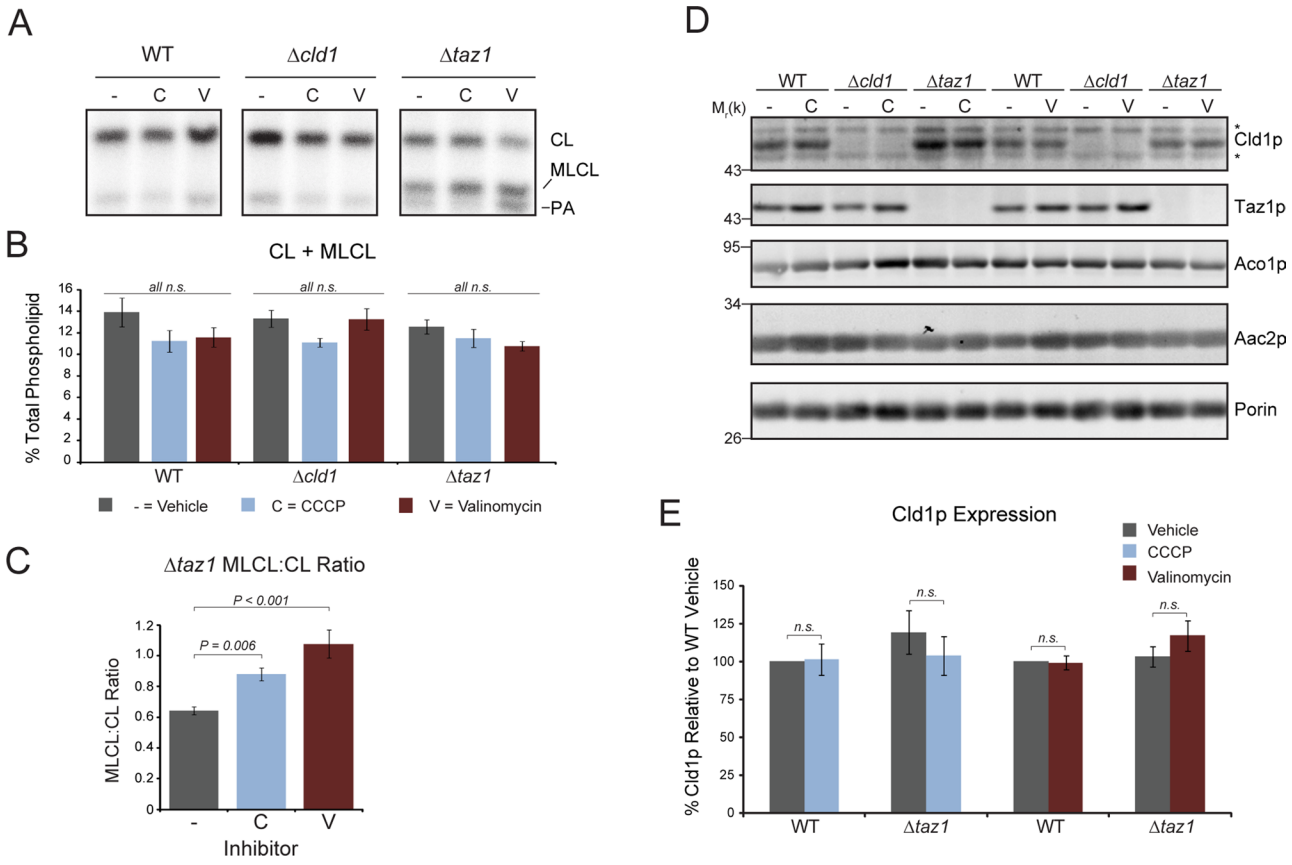

FIGURE 8: Dissipation of the mitochondrial membrane potential promotes Cld1p function. (A) Mitochondrial phospholipids from yeast grown in YP-raffinose spiked with $^{32}P_i$ in the presence of 20 μM CCCP (C), 1 μM valinomycin (V), or vehicle only (–) for 24 h were separated by TLC. (B) The sum of CL + MLCL from the indicated strains (mean ± SEM; $n = 6$). n.s., differences not significant as determined by one-way ANOVA. (C) The ratio of MLCL:CL from Δ*taz1* (mean ± SEM; $n = 6$). Significant differences determined by one-way ANOVA. (D) Whole-cell extracts from the indicated strains grown in the presence of CCCP, valinomycin, or vehicle alone for 24 h were resolved by SDS–PAGE and immunoblotted as indicated. *, nonspecific cross-reactions of the Cld1p antiserum. (E) Cld1p band intensities were quantified and plotted as the % Cld1p relative to wild-type grown in the absence of either ionophore (mean ± SEM; $n = 5$). n.s., differences not significant as determined by *t* test.

(Gallet *et al.*, 1997, 1999); however, the player(s) responsible have not been identified.

A novel link between CL remodeling and OXPHOS

CL biosynthesis is known to be modulated in yeast by the available carbon source; CL levels are decreased in dextrose and increased in nonfermentable carbon sources (Figure 6D; Shen and Dowhan, 1998; Gu *et al.*, 2004; Su and Dowhan, 2006; Chen *et al.*, 2008; Claypool *et al.*, 2008a). Additionally, decreasing the matrix pH reduces Crd1p function, in turn decreasing the steady-state levels of CL (Gohil *et al.*, 2004). In this study, we show that the sum of CL + MLCL, an indicator of CL biosynthesis, is decreased in dextrose compared with raffinose and lactate. Importantly, no difference in CL + MLCL levels is observed between wild-type, Δ*cld1*, and Δ*taz1* yeast, indicating that the differences observed between the various carbon sources are the result of regulation at the level of CL biosynthesis, not remodeling.

In contrast, nothing is known about the regulation of CL remodeling. To investigate this important issue, we addressed three specific questions: 1) Is the CL remodeling pathway regulated? 2) If yes, is there a particular step in the pathway that serves as the master regulator? 3) Is CL remodeling regulated in a manner similar to or distinct from CL biosynthesis?

Cld1p and Taz1p expression is increased approximately twofold in lactate compared with raffinose, despite no difference in CL + MLCL levels. Cld1p, but not Taz1p, expression is repressed in dextrose, consistent with the reduced steady-state levels of CL + MLCL. These observations indicate that Cld1p expression is not exclusively coordinated by CL steady-state levels. More importantly, they indicate that the abundance of CL remodeling enzymes is regulated by the available carbon source.

The MLCL:CL ratio in Δ*taz1* yeast, a measure of Cld1p function, is decreased in dextrose and increased in lactate, correlating with the steady-state expression level of Cld1p. By itself, these data suggest that Cld1p function is regulated by the steady-state abundance of the Cld1p polypeptide. However, overexpression of Cld1p did not result in a proportional increase in the MLCL:CL ratio, suggesting additional modes of Cld1p regulation.

While the presence of various carbon sources and the treatment with ionophores modulates CL remodeling, neither alteration resulted in the accumulation of MLCL in wild-type compared with Δ*cld1*. Thus, the activity of both Taz1p and the unidentified MLCL trafficking protein(s) was not limiting. Of note, Taz1p expression increased after treatment with valinomycin (Figure S4C), suggesting that its expression is modulated to match the rate of CL remodeling. Further, Taz1p expression is not increased due to an increase in its

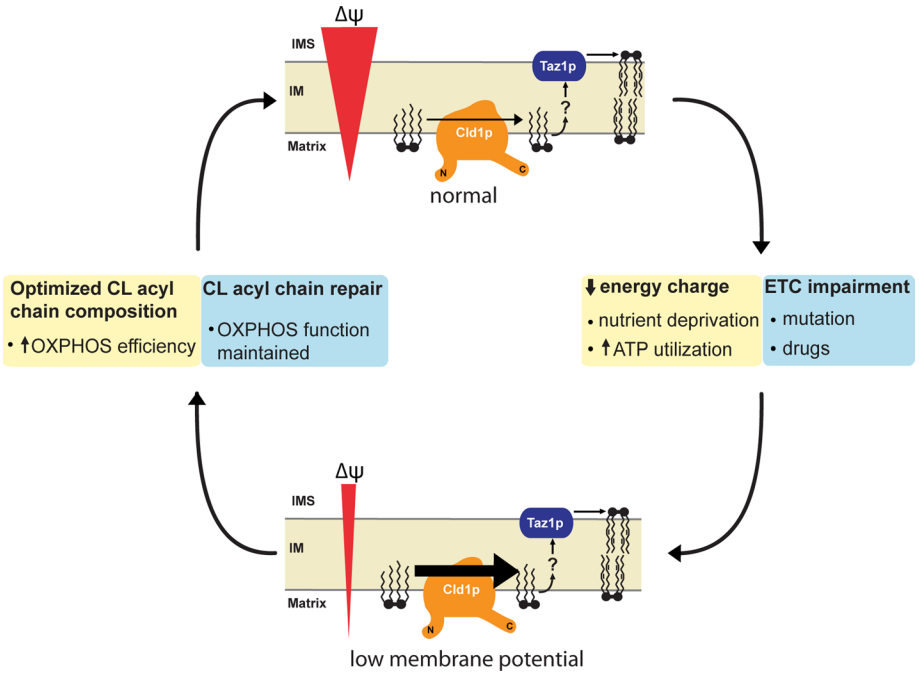

FIGURE 9: A feedback loop between OXPHOS and CL remodeling. CL remodeling is enhanced upon dissipation of the mitochondrial membrane potential (Δψ). Two potential underlying causes for a drop in the mitochondrial membrane potential include: 1) A decreased energy charge (yellow boxes) or 2) impairment of the electron transport chain (ETC), either through mutation or pharmacological insult (blue boxes). A reduced mitochondrial membrane potential will increase the rate of CL remodeling. The resultant additional mature CL may increase the efficiency of OXPHOS and thus reestablish the Δψ (yellow boxes). Alternatively, the increased production of ROS that occurs when proton pumping by the electron transport chain is reduced/impaired may oxidize CL. The increased rate of CL remodeling stimulated by the associated reduction in Δψ may therefore replace oxidized acyl chains in CL with new acyl chains, thus preserving OXPHOS function (blue boxes).

substrate MLCL, because similar increases in Taz1p expression occur in both wild-type and Δ*cld1* after treatment with valinomycin. In sum, these results indicate that removal of an acyl chain from CL by Cld1p represents the major site of regulation for the CL remodeling pathway.

CCCP, a H^+ ionophore, dissipates the mitochondrial membrane potential and decreases the matrix pH, whereas valinomycin, a K^+ ionophore, decreases the membrane potential while maintaining the matrix pH (Gohil *et al.*, 2004). Treatment of yeast for 24 h with a nonlethal concentration of either ionophore did not result in a significant alteration of CL + MLCL levels (Figure 8B; the observed decrease was not statistically significant). This is in contrast to another study that reported a decrease in CL synthesis after treatment with CCCP (Gohil *et al.*, 2004), although phospholipids were pulse-labeled and yeast was treated with ionophores for a shorter time period in these experiments. In Δ*taz1* yeast, the MLCL:CL ratio increased after treatment with either CCCP or valinomycin, despite unchanged expression of Cld1p. Both ionophores decrease the membrane potential, but only CCCP affects the matrix pH; thus Cld1p function increases as the membrane potential decreases.

Taken together, these data indicate that CL remodeling can be regulated by two different mechanisms. First, Cld1p expression (and thus overall function) is regulated by the available carbon source, in a manner similar to the regulation of CL biosynthesis (Shen and Dowhan, 1998; Gu *et al.*, 2004; Su and Dowhan, 2006; Chen *et al.*, 2008; Claypool *et al.*, 2008a), which may allow CL biosynthesis and remodeling rates to be coordinated. Second, Cld1p function is regulated by changes in the mitochondrial membrane potential, representing a regulatory mechanism distinct from that of Crd1p (Gohil *et al.*, 2004) and suggesting that a cell can individually fine-tune both the total levels of CL and the molecular form of CL.

There are at least two non–mutually exclusive benefits of having flux through the CL remodeling pathway regulated by the strength of the membrane potential across the IM (Figure 9). First, physiologically, decreases in the mitochondrial membrane potential indicate greater energetic demand (Huttemann *et al.*, 2008). Essentially, this is a simple way for the cell to coordinate energy production with energy demand. For instance, when cytosolic ATP is depleted, the relative concentration of ADP increases; condensation of ADP and P_i by the ATP synthase is coupled to the downhill flow of protons across the IM through the F_o section, which dissipates the membrane potential (the process of respiratory control; Chance and Williams, 1955). CL remodeling has been proposed to generate a form of CL that functions more optimally than newly synthesized CL (Schlame *et al.*, 2005; Cheng *et al.*, 2008; Claypool and Koehler, 2012). If true, then augmenting Cld1p activity upon dissipation of the membrane potential would increase the relative abundance of remodeled CL, in turn promoting the enhanced activity of the OXPHOS machinery. This novel potential feedback mechanism would therefore link energetic demand with the capacity to produce energy by altering the acyl chain composition of CL.

Second, mitochondria are the major producers of cellular reactive oxygen species (ROS). CL is intimately associated with all of the main players involved in OXPHOS and is susceptible to oxidation (Kim *et al.*, 2011). Further, peroxidized CL inactivates complex IV (Musatov, 2006). Defects in the respiratory chain, either from mutation or through pharmacological insult, have been shown to increase ROS production and decrease the membrane potential (Grivennikova and Vinogradov, 2006; Minners *et al.*, 2007; Quinlan *et al.*, 2011; Baile and Claypool, 2013). Therefore CL remodeling could be activated as part of a mitochondrial ripple-response cascade (Vafai and Mootha, 2012), maintaining OXPHOS capacity by repairing damaged CL molecules. The dissipation of the membrane potential would act as a signal to activate CL remodeling, removing oxidatively damaged acyl chains from CL by Cld1p and replacing them with unadulterated acyl chains by tafazzin-mediated transacylation. In this scenario, OXPHOS capacity would be maintained but not necessarily enhanced by fixing damaged CL molecules, providing a mechanism whereby the membrane potential is reestablished. This in turn would prevent more drastic downstream consequences associated with severe reductions in the membrane potential, including mitophagy or apoptosis (Clayton *et al.*, 2005; Frezza *et al.*, 2006; Twig *et al.*, 2008; Jin *et al.*, 2010). Consistent with this model, oxidative damage is increased in the absence of tafazzin in yeast (Chen *et al.*, 2008) and humans (Gonzalvez *et al.*, 2013), implicating CL remodeling in reducing ROS formation.

MATERIALS AND METHODS

Yeast strains and growth conditions

All strains were derived from the wild-type parental *Saccharomyces cerevisiae* strain GA74-1A (*MAT***a**, *his3-11,15, leu2, ura3, trp1, ade8, rho*$^+$, *mit*$^+$). Δ*crd1* (*MAT***a**, *his3-11,15, leu2, ura3, ade8,* Δ*crd1*::*TRP1*) has been described previously (Claypool *et al.*, 2008b). Δ*cld1* (*MAT***a**, *leu2, ura3, trp1, ade8,* Δ*cld1*::*HIS3MX6*), Δ*taz1* (*MAT***a**, *his3-11,15, leu2, trp1, ade8,* Δ*taz1*::*URA3MX*), and Δ*cld1*Δ*taz1* (*MAT***a**, *leu2, trp1, ade8,* Δ*cld1*::*HIS3MX6,* Δ*taz1*::*URA3MX*) were generated by replacing the entire open reading frame of the gene using PCR-mediated gene replacement (Wach *et al.*, 1994).

Yeast were grown in YP media (1% yeast extract, 2% peptone) supplemented with either 2% dextrose or 2% raffinose in Figures 6 and 8; synthetic dropout media (0.17% yeast nitrogen base, 0.5% ammonium sulfate, 0.2% dropout mix synthetic –leu) supplemented with 2% dextrose or 2% raffinose in Figure 7; synthetic rich lactate –leu (0.17% yeast nitrogen base minus amino acids and ammonium sulfate, 0.5% ammonium sulfate, 0.2% dropout mix synthetic –leu, 0.05% dextrose, 2% lactic acid, 3.4 mM $CaCl_2$–$2H_2O$, 8.5 mM NaCl, 2.95 mM $MgCl_2$–$6H_2O$, 7.35 mM KH_2PO_4, 18.7 mM NH_4Cl, pH 5.5) in Figures 2, 4, 5, and 7; and rich lactate media (1% yeast extract, 2% tryptone, 0.05% dextrose, 2% lactic acid, 3.4 mM $CaCl_2$–$2H_2O$, 8.5 mM NaCl, 2.95 mM $MgCl_2$–$6H_2O$, 7.35 mM KH_2PO_4, 18.7 mM NH_4Cl, pH 5.5) in all other experiments.

For treatment with ionophores, overnight cultures grown in YP-raffinose or rich lactate were diluted to 0.4 OD_{600}/ml in YP-raffinose or rich lactate containing 20 μM CCCP, 1 μM valinomycin, or an equal volume of vehicle (ethanol for CCCP; dimethyl sulfoxide for valinomycin). For growth analysis, the OD_{600} was measured at 0, 2, 4, 6, 8, and 24 h. Phospholipid steady-state levels and protein expression were analyzed after 24 h of treatment.

Molecular biology

CLD1 was amplified from genomic DNA isolated from GA74-1A yeast using primers that hybridized ~450 base pairs 5′ of the predicted start codon and ~100 base pairs 3′ of the predicted stop codon and subcloned into pRS315. *CLD1* point mutations and both the mature N- and C-terminal CNAP-tagged *CLD1* were generated by overlap extension (Ho *et al.*, 1989) using pRS315CLD1 as a template.

Digitonin-based submitochondrial localization

Digitonin-based submitochondrial localization was performed as described previously (Glick *et al.*, 1992; Tamura *et al.*, 2012). Briefly, 250 μg of mitochondria was resuspended in SEHK buffer (250 mM sucrose, 5 mM EDTA, 10 mM HEPES-KOH, pH7.4, 50 mM KCl, 200 μM PMSF) supplemented with 0–0.5% (wt/vol) digitonin and solubilized for 60 s. Cold SEHK buffer (8.5 volumes) was added to stop solubilization. Released proteins were separated from the membrane pellet by centrifugation at 100,000 × *g* (TLA120.1 rotor) for 10 min at 4°C. The supernatant fraction was trichloroacetic acid (TCA)-precipitated, and both supernatant and membrane pellet fractions were resuspended in equal volumes of sample buffer. After separation by SDS–PAGE and immunoblotting as indicated, band intensities were captured with the FluorChem Q (Cell Biosciences, Santa Clara, CA) quantitative digital imaging system and quantified using affiliated AlphaView SA.

Sonication

Mitochondria (500 μg) were osmotically shocked by being resuspended in mitoplasting buffer (30 mM sorbitol, 20 mM HEPES, pH 7.4) and incubated on ice for 30 min. IMS proteins were released by adding KCl in mitoplasting buffer to a final concentration of 0–1 M and being incubated on ice for 15 min. Released proteins (IMS fraction) were separated from mitoplasts by centrifugation at 21,000 × *g* for 10 min at 4°C and TCA-precipitated. Mitoplast pellets were resuspended to 10 mg/ml in sonication buffer (0.6 M sucrose, 3 mM $MgCl_2$, 20 mM HEPES, pH 7.4) containing 0–1 M KCl, and sonicated 3 × 10 s with 30-s intervals using a Sonic Dismembrator 500 (Fisher Scientific, Lafayette, CO) at amplitude 15%. After removal of unbroken mitoplasts by centrifugation, the supernatant was separated from the membrane pellet by centrifugation at 100,000 × *g* for 30 min at 4°C (TLA120.1 rotor), and the supernatant was TCA-precipitated. Equal volumes of each fraction were resolved by SDS–PAGE and immunoblotted. When the IMS fraction was not analyzed, 500 μg of mitochondria was collected by centrifugation, resuspended to 10 mg/ml in sonication buffer, and treated as described above.

Antibodies

Most antibodies used in this study were generated in the Schatz (J. Schatz, Univeristy of Basel, Basel, Switzerland) or Koehler (C. Koehler, University of California, Los Angeles, Los Angeles, CA) laboratories and have been described previously (Daum *et al.*, 1982; Riezman *et al.*, 1983; Claypool *et al.*, 2006, 2008a, 2011; Hwang *et al.*, 2007; Whited *et al.*, 2012). Antibodies against Cld1p, Cox4p, Rip1p, and Qcr6p were raised in rabbits using purified recombinant proteins as antigens. The specificity of each antibody is provided in Figure S5. Recombinant proteins were generated essentially as previously described (Claypool *et al.*, 2006, 2011) by cloning the entire open reading frame into the pET28a vector (Novagen, Darmstadt, Germany) downstream of the 6xHis tag; induced in BL21-CodonPlus(DE3)-RIL *Escherichia coli*; and purified using Ni^{2+} agarose (Qiagen, Valencia, CA). Other antibodies used were mouse anti-Sec62p (a gift from D. Meyers, University of California, Los Angeles, Los Angeles, CA), mouse anti-Aac2p clone 6H8 (Panneels *et al.*, 2003), mouse anti–protein C (Roche, Indianapolis, IN), and horseradish peroxidase–conjugated (Thermo Fisher Scientific, Lafayette, CO) or fluorescence-conjugated (Pierce, Rockford, IL) secondary antibodies.

Miscellaneous

Isolation of mitochondria, subcellular fractionation, preparation of yeast cell extracts, two-dimensional blue native/SDS–PAGE, phospholipid analyses, and immunoblotting were performed as previously described (Claypool *et al.*, 2006, 2008a). Carbonate extraction was performed as previously described (Claypool *et al.*, 2006), except that the pellet and supernatant fractions were separated by centrifugation at 175,000 × *g* for 15 min at 4°C using a TLA120.1 rotor. The proteinase K (PK) accessibility assay was performed as previously described (Claypool *et al.*, 2006), except that 0.5% (wt/vol) deoxycholate was used to solubilize the IM. Phosphate quantification was performed as previously described (Rouser *et al.*, 1970). The homology model of the α/β-hydrolase domain of Cld1p was generated using the SWISS-MODEL Workspace (Guex and Peitsch, 1997; Schwede *et al.*, 2003; Arnold *et al.*, 2006). The predicted mature N-terminus of Cld1p was determined using MitoProt II v1.101 (Claros and Vincens, 1996). Statistical comparisons were performed by *t* test or one-way analysis of variance (ANOVA) with Holm-Sidak pairwise comparison using SigmaPlot 11 software (Systat Software, San Jose, CA).

ACKNOWLEDGMENTS

We thank members of the Claypool lab for critical reading of the manuscript and Jeff Schatz and Carla Koehler for antibodies. This work was supported by National Institutes of Health Grant R00HL089185 (S.M.C.). M.G.B. is a predoctoral fellow of the American Heart Association.

REFERENCES

Acehan D, Khuchua Z, Houtkooper RH, Malhotra A, Kaufman J, Vaz FM, Ren M, Rockman HA, Stokes DL, Schlame M (2009). Distinct effects of tafazzin deletion in differentiated and undifferentiated mitochondria. Mitochondrion 9, 86–95.

Acehan D, Malhotra A, Xu Y, Ren M, Stokes DL, Schlame M (2011). Cardiolipin affects the supramolecular organization of ATP synthase in mitochondria. Biophys J 100, 2184–2192.

Acehan D, Xu Y, Stokes DL, Schlame M (2007). Comparison of lymphoblast mitochondria from normal subjects and patients with Barth syndrome using electron microscopic tomography. Lab Invest 87, 40–48.

Arnold K, Bordoli L, Kopp J, Schwede T (2006). The SWISS-MODEL workspace: a web-based environment for protein structure homology modelling. Bioinformatics 22, 195–201.

Baile MG, Claypool SM (2013). The power of yeast to model diseases of the powerhouse of the cell. Front Biosci 18, 241–278.

Ban T, Heymann JA, Song Z, Hinshaw JE, Chan DC (2010). OPA1 disease alleles causing dominant optic atrophy have defects in cardiolipin-stimulated GTP hydrolysis and membrane tubulation. Hum Mol Genet 19, 2113–2122.

Barth PG, Scholte HR, Berden JA, Van der Klei-Van Moorsel JM, Luyt-Houwen IE, Van 't Veer-Korthof ET, Van der Harten JJ, Sobotka-Plojhar MA (1983). An X-linked mitochondrial disease affecting cardiac muscle, skeletal muscle and neutrophil leucocytes. J Neurol Sci 62, 327–355.

Beranek A, Rechberger G, Knauer H, Wolinski H, Kohlwein SD, Leber R (2009). Identification of a cardiolipin-specific phospholipase encoded by the gene *CLD1* (*YGR110W*) in yeast. J Biol Chem 284, 11572–11578.

Bione S, D'Adamo P, Maestrini E, Gedeon AK, Bolhuis PA, Toniolo D (1996). A novel X-linked gene, *G4.5*. is responsible for Barth syndrome. Nat Genet 12, 385–389.

Brandner K, Mick DU, Frazier AE, Taylor RD, Meisinger C, Rehling P (2005). Taz1, an outer mitochondrial membrane protein, affects stability and assembly of inner membrane protein complexes: implications for Barth syndrome. Mol Biol Cell 16, 5202–5214.

Carr PD, Ollis DL (2009). Alpha/beta hydrolase fold: an update. Protein Pept Lett 16, 1137–1148.

Chance B, Williams GR (1955). Respiratory enzymes in oxidative phosphorylation. III. The steady state. J Biol Chem 217, 409–427.

Chen S, He Q, Greenberg ML (2008). Loss of tafazzin in yeast leads to increased oxidative stress during respiratory growth. Mol Microbiol 68, 1061–1072.

Cheng H, Mancuso DJ, Jiang X, Guan S, Yang J, Yang K, Sun G, Gross RW, Han X (2008). Shotgun lipidomics reveals the temporally dependent, highly diversified cardiolipin profile in the mammalian brain: temporally coordinated postnatal diversification of cardiolipin molecular species with neuronal remodeling. Biochemistry 47, 5869–5880.

Claros MG, Vincens P (1996). Computational method to predict mitochondrially imported proteins and their targeting sequences. Eur J Biochem 241, 779–786.

Claypool SM, Boontheung P, McCaffery JM, Loo JA, Koehler CM (2008a). The cardiolipin transacylase, tafazzin, associates with two distinct respiratory components providing insight into Barth syndrome. Mol Biol Cell 19, 5143–5155.

Claypool SM, Koehler CM (2012). The complexity of cardiolipin in health and disease. Trends Biochem Sci 37, 32–41.

Claypool SM, McCaffery JM, Koehler CM (2006). Mitochondrial mislocalization and altered assembly of a cluster of Barth syndrome mutant tafazzins. J Cell Biol 174, 379–390.

Claypool SM, Oktay Y, Boontheung P, Loo JA, Koehler CM (2008b). Cardiolipin defines the interactome of the major ADP/ATP carrier protein of the mitochondrial inner membrane. J Cell Biol 182, 937–950.

Claypool SM, Whited K, Srijumnong S, Han X, Koehler CM (2011). Barth syndrome mutations that cause tafazzin complex lability. J Cell Biol 192, 447–462.

Clayton R, Clark JB, Sharpe M (2005). Cytochrome *c* release from rat brain mitochondria is proportional to the mitochondrial functional deficit: implications for apoptosis and neurodegenerative disease. J Neurochem 92, 840–849.

Connerth M, Tatsuta T, Haag M, Klecker T, Westermann B, Langer T (2013). Intramitochondrial transport of phosphatidic acid in yeast by a lipid transfer protein. Science 338, 815–818.

Daum G, Bohni PC, Schatz G (1982). Import of proteins into mitochondria. Cytochrome b_2 and cytochrome *c* peroxidase are located in the intermembrane space of yeast mitochondria. J Biol Chem 257, 13028–13033.

DeVay RM, Dominguez-Ramirez L, Lackner LL, Hoppins S, Stahlberg H, Nunnari J (2009). Coassembly of Mgm1 isoforms requires cardiolipin and mediates mitochondrial inner membrane fusion. J Cell Biol 186, 793–803.

Dzugasova V, Obernauerova M, Horvathova K, Vachova M, Zakova M, Subik J (1998). Phosphatidylglycerolphosphate synthase encoded by the *PEL1/PGS1* gene in *Saccharomyces cerevisiae* is localized in mitochondria and its expression is regulated by phospholipid precursors. Curr Genet 34, 297–302.

Eble KS, Coleman WB, Hantgan RR, Cunningham CC (1990). Tightly associated cardiolipin in the bovine heart mitochondrial ATP synthase as analyzed by 31P nuclear magnetic resonance spectroscopy. J Biol Chem 265, 19434–19440.

Frezza C *et al.* (2006). OPA1 controls apoptotic cristae remodeling independently from mitochondrial fusion. Cell 126, 177–189.

Fry M, Green DE (1980). Cardiolipin requirement by cytochrome oxidase and the catalytic role of phospholipid. Biochem Biophys Res Commun 93, 1238–1246.

Fry M, Green DE (1981). Cardiolipin requirement for electron transfer in complex I and III of the mitochondrial respiratory chain. J Biol Chem 256, 1874–1880.

Fushinobu S, Saku T, Hidaka M, Jun SY, Nojiri H, Yamane H, Shoun H, Omori T, Wakagi T (2002). Crystal structures of a *meta*-cleavage product hydrolase from *Pseudomonas fluorescens* IP01 (CumD) complexed with cleavage products. Protein Sci 11, 2184–2195.

Gallet PF, Petit JM, Maftah A, Zachowski A, Julien R (1997). Asymmetrical distribution of cardiolipin in yeast inner mitochondrial membrane triggered by carbon catabolite repression. Biochem J 324, 627–634.

Gallet PF, Zachowski A, Julien R, Fellmann P, Devaux PF, Maftah A (1999). Transbilayer movement and distribution of spin-labelled phospholipids in the inner mitochondrial membrane. Biochim Biophys Acta 1418, 61–70.

Gebert N *et al.* (2009). Mitochondrial cardiolipin involved in outer-membrane protein biogenesis: implications for Barth syndrome. Curr Biol 19, 2133–2139.

Glick BS, Brandt A, Cunningham K, Muller S, Hallberg RL, Schatz G (1992). Cytochromes c_1 and b_2 are sorted to the intermembrane space of yeast mitochondria by a stop-transfer mechanism. Cell 69, 809–822.

Gohil VM, Hayes P, Matsuyama S, Schagger H, Schlame M, Greenberg ML (2004). Cardiolipin biosynthesis and mitochondrial respiratory chain function are interdependent. J Biol Chem 279, 42612–42618.

Gomez B Jr., Robinson NC (1999). Phospholipase digestion of bound cardiolipin reversibly inactivates bovine cytochrome bc_1. Biochemistry 38, 9031–9038.

Gonzalvez F *et al.* (2013). Barth syndrome: cellular compensation of mitochondrial dysfunction and apoptosis inhibition due to changes in cardiolipin remodeling linked to tafazzin gene mutation. Biochim Biophys Acta 1832, 1194–1206.

Gonzalvez F, Schug ZT, Houtkooper RH, MacKenzie ED, Brooks DG, Wanders RJ, Petit PX, Vaz FM, Gottlieb E (2008). Cardiolipin provides an essential activating platform for caspase-8 on mitochondria. J Cell Biol 183, 681–696.

Grivennikova VG, Vinogradov AD (2006). Generation of superoxide by the mitochondrial complex I. Biochim Biophys Acta 1757, 553–561.

Gu Z, Valianpour F, Chen S, Vaz FM, Hakkaart GA, Wanders RJ, Greenberg ML (2004). Aberrant cardiolipin metabolism in the yeast taz1 mutant: a model for Barth syndrome. Mol Microbiol 51, 149–158.

Guex N, Peitsch MC (1997). SWISS-MODEL and the Swiss-PdbViewer: an environment for comparative protein modeling. Electrophoresis 18, 2714–2723.

Ho SN, Hunt HD, Horton RM, Pullen JK, Pease LR (1989). Site-directed mutagenesis by overlap extension using the polymerase chain reaction. Gene 77, 51–59.

Holmquist M (2000). Alpha/beta-hydrolase fold enzymes: structures, functions and mechanisms. Curr Protein Pept Sci 1, 209–235.

Horvath SE, Bottinger L, Vogtle FN, Wiedemann N, Meisinger C, Becker T, Daum G (2012). Processing and topology of the yeast mitochondrial phosphatidylserine decarboxylase 1. J Biol Chem 287, 36744–36755.

Huttemann M, Lee I, Pecinova A, Pecina P, Przyklenk K, Doan JW (2008). Regulation of oxidative phosphorylation, the mitochondrial membrane potential, and their role in human disease. J Bioenerg Biomembr 40, 445–456.

Hwang DK, Claypool SM, Leuenberger D, Tienson HL, Koehler CM (2007). Tim54p connects inner membrane assembly and proteolytic pathways in the mitochondrion. J Cell Biol 178, 1161–1175.

Jiang F, Rizavi HS, Greenberg ML (1997). Cardiolipin is not essential for the growth of *Saccharomyces cerevisiae* on fermentable or non-fermentable carbon sources. Mol Microbiol 26, 481–491.
Jiang F, Ryan MT, Schlame M, Zhao M, Gu Z, Klingenberg M, Pfanner N, Greenberg ML (2000). Absence of cardiolipin in the *crd1* null mutant results in decreased mitochondrial membrane potential and reduced mitochondrial function. J Biol Chem 275, 22387–22394.
Jin SM, Lazarou M, Wang C, Kane LA, Narendra DP, Youle RJ (2010). Mitochondrial membrane potential regulates PINK1 import and proteolytic destabilization by PARL. J Cell Biol 191, 933–942.
Kim J, Minkler PE, Salomon RG, Anderson VE, Hoppel CL (2011). Cardiolipin: characterization of distinct oxidized molecular species. J Lipid Res 52, 125–135.
Kim KK, Song HK, Shin DH, Hwang KY, Choe S, Yoo OJ, Suh SW (1997). Crystal structure of carboxylesterase from *Pseudomonas fluorescens*, an alpha/beta hydrolase with broad substrate specificity. Structure 5, 1571–1584.
Koshkin V, Greenberg ML (2000). Oxidative phosphorylation in cardiolipin-lacking yeast mitochondria. Biochem J 347, 687–691.
Kuge O, Nishijima M (2003). Biosynthetic regulation and intracellular transport of phosphatidylserine in mammalian cells. J Biochem 133, 397–403.
Li J *et al*. (2010). Cardiolipin remodeling by ALCAT1 links oxidative stress and mitochondrial dysfunction to obesity. Cell Metab 12, 154–165.
Malhotra A, Xu Y, Ren M, Schlame M (2009). Formation of molecular species of mitochondrial cardiolipin. 1. A novel transacylation mechanism to shuttle fatty acids between sn-1 and sn-2 positions of multiple phospholipid species. Biochim Biophys Acta 1791, 314–320.
Marom M, Safonov R, Amram S, Avneon Y, Nachliel E, Gutman M, Zohary K, Azem A, Tsfadia Y (2009). Interaction of the Tim44 C-terminal domain with negatively charged phospholipids. Biochemistry 48, 11185–11195.
Minners J, Lacerda L, Yellon DM, Opie LH, McLeod CJ, Sack MN (2007). Diazoxide-induced respiratory inhibition—a putative mitochondrial K(ATP) channel independent mechanism of pharmacological preconditioning. Mol Cell Biochem 294, 11–18.
Montessuit S *et al*. (2010). Membrane remodeling induced by the dynamin-related protein Drp1 stimulates Bax oligomerization. Cell 142, 889–901.
Musatov A (2006). Contribution of peroxidized cardiolipin to inactivation of bovine heart cytochrome *c* oxidase. Free Radic Biol Med 41, 238–246.
Ohlmeier S, Kastaniotis AJ, Hiltunen JK, Bergmann U (2004). The yeast mitochondrial proteome, a study of fermentative and respiratory growth. J Biol Chem 279, 3956–3979.
Osman C, Haag M, Wieland FT, Brugger B, Langer T (2010). A mitochondrial phosphatase required for cardiolipin biosynthesis: the PGP phosphatase Gep4. EMBO J 29, 1976–1987.
Ostrander DB, Sparagna GC, Amoscato AA, McMillin JB, Dowhan W (2001). Decreased cardiolipin synthesis corresponds with cytochrome *c* release in palmitate-induced cardiomyocyte apoptosis. J Biol Chem 276, 38061–38067.
Panneels V, Schussler U, Costagliola S, Sinning I (2003). Choline head groups stabilize the matrix loop regions of the ATP/ADP carrier ScAAC2. Biochem Biophys Res Commun 300, 65–74.
Petit JM, Huet O, Gallet PF, Maftah A, Ratinaud MH, Julien R (1994). Direct analysis and significance of cardiolipin transverse distribution in mitochondrial inner membranes. Eur J Biochem 220, 871–879.
Pfeiffer K, Gohil V, Stuart RA, Hunte C, Brandt U, Greenberg ML, Schagger H (2003). Cardiolipin stabilizes respiratory chain supercomplexes. J Biol Chem 278, 52873–52880.
Quinlan CL, Gerencser AA, Treberg JR, Brand MD (2011). The mechanism of superoxide production by the antimycin-inhibited mitochondrial Q-cycle. J Biol Chem 286, 31361–31372.
Riezman H, Hay R, Gasser S, Daum G, Schneider G, Witte C, Schatz G (1983). The outer membrane of yeast mitochondria: isolation of outside-out sealed vesicles. EMBO J 2, 1105–1111.
Rouser G, Fkeischer S, Yamamoto A (1970). Two dimensional thin layer chromatographic separation of polar lipids and determination of phospholipids by phosphorus analysis of spots. Lipids 5, 494–496.
Schlame M, Acehan D, Berno B, Xu Y, Valvo S, Ren M, Stokes DL, Epand RM (2012). The physical state of lipid substrates provides transacylation specificity for tafazzin. Nat Chem Biol 8, 862–869.
Schlame M, Haldar D (1993). Cardiolipin is synthesized on the matrix side of the inner membrane in rat liver mitochondria. J Biol Chem 268, 74–79.
Schlame M, Kelley RI, Feigenbaum A, Towbin JA, Heerdt PM, Schieble T, Wanders RJ, DiMauro S, Blanck TJ (2003). Phospholipid abnormalities in children with Barth syndrome. J Am Coll Cardiol 42, 1994–1999.
Schlame M, Ren M (2006). Barth syndrome, a human disorder of cardiolipin metabolism. FEBS Lett 580, 5450–5455.
Schlame M, Ren M, Xu Y, Greenberg ML, Haller I (2005). Molecular symmetry in mitochondrial cardiolipins. Chem Phys Lipids 138, 38–49.
Schlame M, Rua D, Greenberg ML (2000). The biosynthesis and functional role of cardiolipin. Prog Lipid Res 39, 257–288.
Schwall CT, Greenwood VL, Alder NN (2012). The stability and activity of respiratory complex II is cardiolipin-dependent. Biochim Biophys Acta 1817, 1588–1596.
Schwede T, Kopp J, Guex N, Peitsch MC (2003). SWISS-MODEL: An automated protein homology-modeling server. Nucleic Acids Res 31, 3381–3385.
Sedlak E, Robinson NC (1999). Phospholipase A(2) digestion of cardiolipin bound to bovine cytochrome *c* oxidase alters both activity and quaternary structure. Biochemistry 38, 14966–14972.
Shen H, Dowhan W (1998). Regulation of phosphatidylglycerolphosphate synthase levels in *Saccharomyces cerevisiae*. J Biol Chem 273, 11638–11642.
Su X, Dowhan W (2006). Regulation of cardiolipin synthase levels in *Saccharomyces cerevisiae*. Yeast 23, 279–291.
Tamura Y, Onguka O, Itoh K, Endo T, Iijima M, Claypool SM, Sesaki H (2012). Phosphatidylethanolamine biosynthesis in mitochondria: phosphatidylserine (PS) trafficking is independent of a PS decarboxylase and intermembrane space proteins UPS1P and UPS2P. J Biol Chem 287, 43961–43971.
Taylor WA, Hatch GM (2009). Identification of the human mitochondrial linoleoyl-coenzyme A monolysocardiolipin acyltransferase (MLCL AT-1). J Biol Chem 284, 30360–30371.
Thoms S, Hofhuis J, Thoing C, Gartner J, Niemann HH (2011). The unusual extended C-terminal helix of the peroxisomal α/β-hydrolase Lpx1 is involved in dimer contacts but dispensable for dimerization. J Struct Biol 175, 362–371.
Tuller G, Hrastnik C, Achleitner G, Schiefthaler U, Klein F, Daum G (1998). YDL142c encodes cardiolipin synthase (Cls1p) and is non-essential for aerobic growth of *Saccharomyces cerevisiae*. FEBS Lett 421, 15–18.
Twig G *et al*. (2008). Fission and selective fusion govern mitochondrial segregation and elimination by autophagy. EMBO J 27, 433–446.
Vafai SB, Mootha VK (2012). Mitochondrial disorders as windows into an ancient organelle. Nature 491, 374–383.
Valianpour F *et al*. (2005). Monolysocardiolipins accumulate in Barth syndrome but do not lead to enhanced apoptosis. J Lipid Res 46, 1182–1195.
van der Laan M, Meinecke M, Dudek J, Hutu DP, Lind M, Perschil I, Guiard B, Wagner R, Pfanner N, Rehling P (2007). Motor-free mitochondrial presequence translocase drives membrane integration of preproteins. Nat Cell Biol 9, 1152–1159.
van Meer G, Voelker DR, Feigenson GW (2008). Membrane lipids: where they are and how they behave. Nat Rev Mol Cell Biol 9, 112–124.
Voelker DR (2005). Bridging gaps in phospholipid transport. Trends Biochem Sci 30, 396–404.
Wach A, Brachat A, Pohlmann R, Philippsen P (1994). New heterologous modules for classical or PCR-based gene disruptions in *Saccharomyces cerevisiae*. Yeast 10, 1793–1808.
Whited K, Baile MG, Currier P, Claypool SM (2012). Seven functional classes of Barth syndrome mutation. Hum Mol Genet 22, 483–492.
Xu Y, Kelley RI, Blanck TJ, Schlame M (2003). Remodeling of cardiolipin by phospholipid transacylation. J Biol Chem 278, 51380–51385.
Xu Y, Malhotra A, Ren M, Schlame M (2006). The enzymatic function of tafazzin. J Biol Chem 281, 39217–39224.
Zhang J *et al*. (2011). Mitochondrial phosphatase PTPMT1 is essential for cardiolipin biosynthesis. Cell Metab 13, 690–700.
Zhang M, Mileykovskaya E, Dowhan W (2002). Gluing the respiratory chain together. Cardiolipin is required for supercomplex formation in the inner mitochondrial membrane. J Biol Chem 277, 43553–43556.
Zhang M, Mileykovskaya E, Dowhan W (2005). Cardiolipin is essential for organization of complexes III and IV into a supercomplex in intact yeast mitochondria. J Biol Chem 280, 29403–29408.
Zhong Q, Gohil VM, Ma L, Greenberg ML (2004). Absence of cardiolipin results in temperature sensitivity, respiratory defects, and mitochondrial DNA instability independent of pet56. J Biol Chem 279, 32294–32300.